On topological properties of massless fermions in a magnetic field

Lemut, G.

1 Introduction

1.1 Preface

Electrons are massive, charged, elementary particles with a half-integer spin, that govern the behavior of most atoms and materials. In condensed matter physics, quantum mechanics is used to predict their behavior, leading to remarkable and sometimes counter intuitive phenomena. While free electrons in vacuum are well understood, in condensed matter systems, electrons acquire unusual properties from their interaction with the atomic lattice.

Since the discovery of the mono-layered carbon crystal graphene [1, 2] we know, that they can behave as massless particles called Dirac and Weyl fermions. These exist as low energy excitations giving electrons relativistic behaviour on non-relativistic-scales with a constant velocity analogous to the speed of light. In other systems where superconductivity [3] is present electrons can exhibit transport without resistance as a consequence of a Cooper pair condensate. This allows for exotic Bogoliubov excitations that unlike free electrons are not eigenstates of charge. Under special circumstances such Bogoliubov excitations can mimic special Majorana particles. In these systems electron excitations uniquely act as their own anti-particles [4]. While such states were first predicted in particle physics it turns out that they can be realized as elementary excitations in topological superconductors.

These examples highlight that, despite their apparent simplicity, electrons can exhibit a plethora of fascinating quasi-particle excitations in condensed matter systems. This thesis will examine the interplay of the above mentioned phenomena that arise in robust systems as a consequence of different symmetries as well as topological properties [5]. We will examine how such massless Dirac, Weyl, and Majorana quasi-particles interact with the magnetic field giving rise to new and unique phenomena. In particular, this thesis will examine the formation of zeroth Landau levels in superconducting systems, find transport signatures in Weyl superconductors [6, 7], as well as study a new type of delocalized solutions in the Fu-Kane model [8]. It will explore disordered massless systems, finding new predictions of localized states as well as unique spectral properties. Finally, it will study the recently predicted Kramers-Weyl semimetals [9, 10] and show a new characteristic signature of the magneto-conductance.

While this thesis covers various different realizations of massless systems, the rest of this chapter will focus on introducing two of the most relevant and recently discovered systems. After a brief demonstration how massless fermions can arise in condensed matter system we will firsly show how the interplay between Dirac states in a topological insulator and superconductivity [11, 12] can give rise to the so called Fu-Kane model. This part will describe how such a model can exhibit a transition between a gapped and a gapless phase, as well as how this transition can interplay with the magnetic field to create Majorana excitations. Second, we will focus on a recent realization of three-dimensional Weyl fermions [13], demonstrating their special topological protection and discussing their surface states, which give rise to new characteristic signatures.

1.2 Massless fermions in electronic systems

In the field of condensed matter physics, our focus lies on the study of electrons far away from the relativistic limit. To predict their dynamics, we use the well known Schrödinger equation

$$i\hbar\partial_t\Psi = \left(-\frac{\hbar^2}{2m}\nabla^2 + V\right)\Psi. \tag{1.1}$$

The right-hand side consists of two terms, $-\frac{\hbar^2}{2m}\nabla^2$ represents the kinetic part, while $V(x)$ describes the potential felt by the particles. When the potential term is vanishing, the equation describes free electrons with the well known quadratic dispersion relation

$$E = \frac{p^2}{2m}, \tag{1.2}$$

connecting the energy and momentum. When electrons interact with the environment through the potential $V(x)$, we can no longer write down such a dispersion relation, as momentum is no longer a good quantum number. In condensed matter physics, we are mostly interested in the behaviour of electrons inside crystal structures. These can be described by a periodic potential that arises from the atomic structure. As a consequence of this periodicity, we can define a new quasi-momentum quantum number that forms a translationally invariant eigenspace.This quasi-momentum is restricted to the finite Brillouin zone due to the periodic structure of the potential. In such basisc we can diagonalize the Hamiltonians of crystalline systems and find new quasi-momentum dispersion relations.

For different forms of periodic potentials, the relation between the energies and quasi-momentum can take diverse forms. While the dispersion now has to be periodic, in the simplest example, it still remains effectively quadratic around the center of the Brillouin zone. As the quadratic curvature can change, it can influence low-energy behaviour, altering the effective mass of the low energy excitations. This can give rise to very heavy quasi-particles with a flattened dispersionc as well as light excitations with a vanishing effective mass.

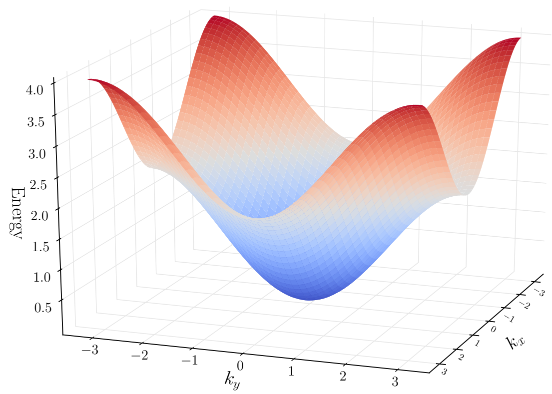

Figure 1.1: Example of a single band tight-binding Cosine dispersion. The dispersion around the minima of the band resembles free electron quadratic dispersion relation with a renormalized effective mass.

When the effective mass of elementary excitations becomes sufficiently small, the corresponding quasi-particles need to be described by a relativistic theory. In this limit, we have to include a spinor degree of freedom to satisfy the relativistic symmetries. These spinors can arise from the various orbital degrees of freedom as well as the actual electron spin. In such systems, we can describe the elementary excitations of electrons, using the full relativistic Dirac equation. In two-dimensional case, this reduces to

$$i\hbar\partial_t\Psi = (v_f\sigma_x k_x + v_f\sigma_y k_y + M_{eff}\sigma_z)\Psi, \tag{1.3}$$

where we have assumed an isotropic Fermi velocity v_f and used σ to denote the two-dimensional Pauli matrices. Such an effective theory describes two species of quasi-particle excitations with symmetric dispersions

$$E_{\pm} = \pm\sqrt{v_f^2 k_x^2 + v_f^2 k_x^2 + M_{\text{eff}}^2}. \tag{1.4}$$

In general, most crystals can exhibit perturbations that keep such an effective mass term finite. In such systems, the quasi-particle dispersion is gapped with a quadratic behaviour for small momentum. However, some crystals exhibit special symmetries that disallow such an effective mass. In such cases, the two bands of the dispersion cross, resulting in a fully gapless quasi-particle dispersion

$$E_{\pm} = \pm v_f|\vec{k}|. \tag{1.5}$$

These special types of quasi-particles, called massless fermions, exhibit a relativistic linear dispersion. They propagate at a constant velocity v_f mimicking the behaviour of photons. Such massless excitations can be generalized to different dimensions, giving rise to Majorana, Dirac and Weyl quasi-particles. While these can arise as a consequence of various crystalline symmetries, their protection can be understood using topological arguments. With these, it is possible to prove the robustness of such emergent relativistic excitations as well as the universality of their unique properties.

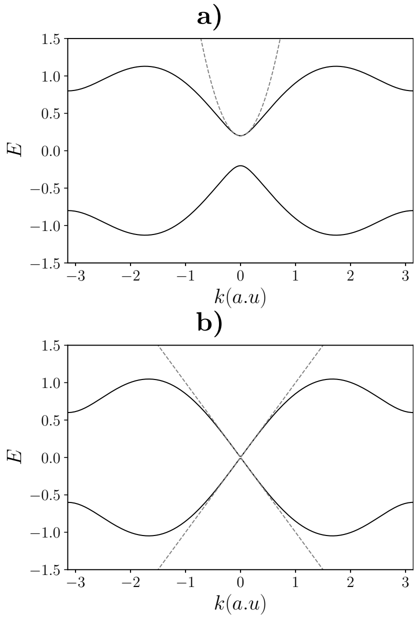

Figure 1.2: (a) Dispersion around an avoided band crossing with a quadratic behaviour around the band minima. (b) An example of a system where the band crossing is protected, giving rise to a gapless point in momentum space with a linear dispersion.

1.3 Dirac fermions to superconducting Majorana excitations

In condensed matter physics, two dimensional massless fermions are called Dirac fermions. They can be described by the two dimensional Dirac equation where a special symmetry prevents the additional mass term. Nature presents us with various mechanisms that can protect these quasi-particle excitations. One of the most famous examples is the single layer carbon crystal graphene where its two gapless Dirac points are protected by an approximate sublattice symmetry arising from the underlying hexagonal lattice.

This thesis explores a more recent realization of Dirac fermions, specifically surface excitations of a three-dimensional topological insulator. In such systems, each surface exhibits a strongly protected Dirac cone due to time-reversal symmetry. We will examine how the interplay between such Dirac states and superconductivity gives rise to the Fu-Kane topological superconductor. While superconductivity in general gaps out the Dirac fermions it is well known that in this model strong supercurrent can be used to restore such gapless points. We have found that such supercurrents can induce another transition in the presence of magnetic field, where Majorana zero-modes extend into a novel extended superconducting state resembling a Landau level. To combine all these ingredients we will first focus on the way the magnetic field affects massless fermions. We will then examine the proximity effect and the Fu-Kane model and finally combine all these ingredients to discuss the Majorana zero energy excitations.

1.3.1 Zeroth Landau level in a 3D topological insulator

We start by introducing the three-dimensional topological insulator. We generally define insulators as non-conducting systems characterized by a large gap around the Fermi energy. Such gapped insulating systems are classified as trivial if they can be continuously transformed into the atomic limit and are therefore topologically equivalent to the vacuum. However, not all insulators can be described in this way. There exists a special type of insulator that cannot be transformed into the atomic limit without closing the band-gap. These systems are called topological insulators and are characterized by special edge states that arise from the gap closing on the interface between the topologically non-trivial insulating bulk and the trivial vacuum. In three dimensions, such topological insulators exhibit two-dimensional surface states, which can be described by the effective surface model

$$H_{\mathrm{TI}} = \tau_z \sigma_x k_x + \tau_z \sigma_y k_y + \tau_x \sigma_0 M(\vec{k}). \tag{1.6}$$

Each surface of the three-dimensional topological insulator, represented by Pauli matrices τ, exhibits a single Dirac fermion coupled together by an effective mass term $M(\vec{k})$. The surfaces become fully decoupled when they are separated from each other. In this limit, each surface exhibits a single Dirac fermion that is protected by the time-reversal symmetry.

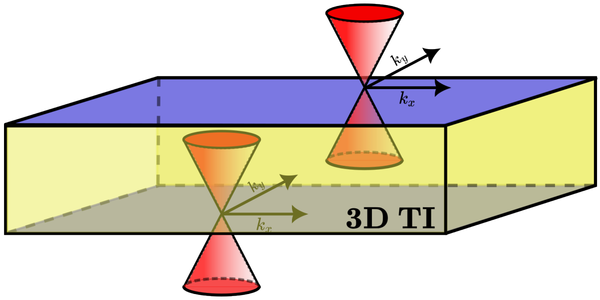

Figure 1.3: Schematic representation of a three-dimensional topological insulator. Each of the two surfaces (blue) exhibits a massless Dirac fermion.

When massless Dirac fermions are subjected to a magnetic field, they exhibit a unique type of energy spectrum. In classical mechanics, charged particles experience a Lorentz force that causes them to move in circular trajectories known as cyclotron orbits. While this intuition can hold down all the way to the quantum level, in quantum mechanics not all such orbits allowed. We call this discrete set of possible states in a magnetic field Landau levels[14]. These levels can be calculated by incorporating the magnetic field into the free particle Schrödinger equation, resulting in a quantized energy spectrum

$$E_n = \hbar\omega_c\left(n + \frac{1}{2}\right), \tag{1.7}$$

where $\omega_c = \frac{eB}{m}$ is the cyclotron frequency and n is a non-negative integer number. When we study massless fermions, the quantization condition changes into

$$E^{LL}_{\text{massless}} = \pm\sqrt{2n\hbar eBv_f^2}, \tag{1.8}$$

where v_f represents the Fermi velocity. The Landau levels are no longer equally spaced and allow for a new type of cyclotron orbits that are bound to exactly zero energy. These states are called zeroth Landau levels.

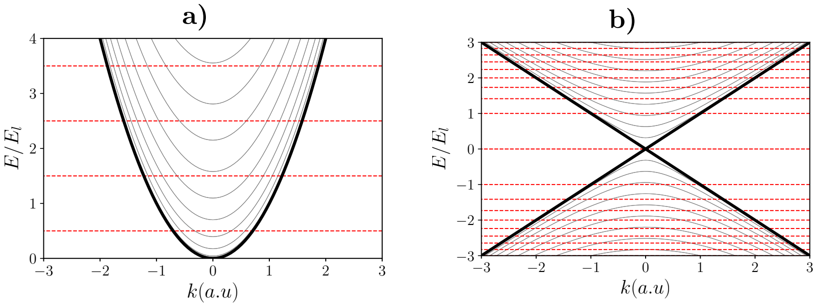

Figure 1.4: The dispersion Landau levels (red) compared to their initial dispersion (gray) for (a) massive and (b) massless particles compared to their initial dispersion.

1.3.2 Proximity effect and the Fu-Kane model

We can now explore what happens to the Dirac surface states under the effect of superconductivity. While there are a number of materials that can exhibit inherent superconducting properties at low temperatures, they usually belong to the class of trivial superconductors. Alternatively, it turns out that creating an interface between a superconducting and non-superconducting material can allow Cooper pair tunneling. This process is called the proximity effect and can induce an effective superconducting pairing. Such proximitized systems can be described by the Bogoliubov-De Gennes Hamiltonian

$$H_{BdG} = \begin{pmatrix} H(\vec{k}) & \Delta \\ \Delta^\dagger & -\mathcal{T}H(\vec{k})\mathcal{T} \end{pmatrix}, \tag{1.9}$$

where Δ denotes the superconducting pairing and $\mathcal{T}$ represents the time-reversal symmetry. This method allows us to describe the mean-field superconducting Hamiltonian by doubling the degrees of freedom. In particular, we artificially add hole-like degrees of freedom to the electronic Hamiltonian and couple them together with a superconducting pairing term Δ. Although superconducting states are not eigenstates of the electron number, this doubling allows us to introduce effective single-particle excitations called the Bogoliubov quasi-particles.

This thesis focuses on a special model of a topological superconductor called the Fu-Kane model. Such systems arise when we create an interface between a three-dimensional topological insulator and a conventional superconductor. In this case, the Bogoliubov De-Gennes doubling creates an additional hole-like Dirac fermion on each surface. The pair of Dirac fermions can now couple through superconducting pairing without violating the time-reversal symmetry. Such coupling gives us the gapped dispersion of the Fu-Kane model.

One of the characteristic signatures of superconductors is a dissipationless current called the supercurrent. This current can be interpreted as the momentum of Cooper pairs. Such a current can split the electron-like and hole-like states in the Brillouin zone. In the particular case of the Fu-Kane heterostructure, this can separate the Dirac fermions in momentum space. We can see this in the Bogoliubov de-Gennes Hamiltonian

$$H_{BdG} = \begin{pmatrix} \left(\vec{k} - \vec{K}\right) \cdot \sigma & \Delta \\ \Delta^\dagger & -\left(\vec{k} + \vec{K}\right) \cdot \sigma \end{pmatrix}, \tag{1.10}$$

in which the supercurrent momentum $\vec{K}$ acts as a constant vector potential. It turns out that such separation slowly decouples the two Dirac fermions. It was shown a sufficient super-current can fully counteract the superconducting pairing creating a transition, restoring the gapless Dirac cone.

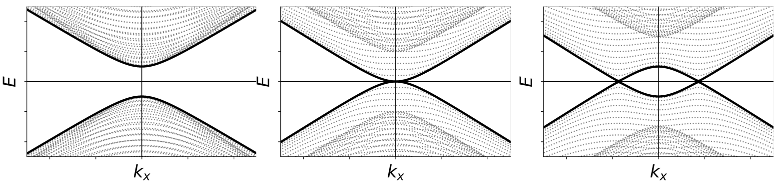

Figure 1.5: Dispersion of a Fu-Kane model with increasing suppercurrent strength (left to right), showing the transition from gapped massive Dirac fermions in a Fu-Kane model to the gapless Dirac states.

1.3.3 Majorana zero-modes in a topological superconductor

In our research, we investigated the effect of a magnetic field on the gap closing transition in the Fu-Kane model. As this is a superconducting system, the effects of a magnetic field can be very different. It is important to note that superconductors exhibit a specific property called the Meissner effect, whereby they expel the effects of magnetic fields. This phenomenon implies that the effects of a magnetic field cannot penetrate a superconductor beyond a certain depth, known as the London penetration length. If we are interested in the effects of a magnetic field on bulk superconductors, we must focus on a specific group of superconductors called type-II superconductors. In this case, the magnetic field penetrates the superconductor in the form of localized defects called Abrikosov vortices[15]. These vortices are strong defects that carry exactly one quantum of magnetic flux, denoted as $\Phi_0 = h/(2e)$. The size of the defects is characterized by the superconducting coherence length, denoted as ξ, which is approximately equal to $1/\Delta_0$, while they carry the flux Φ_0 with circulating supercurrents that persist on a larger scale of the London penetration depth. At the level of wavefunctions, the Abrikosov vortices induce a winding of the superconducting phase parameter around their core by 2π.

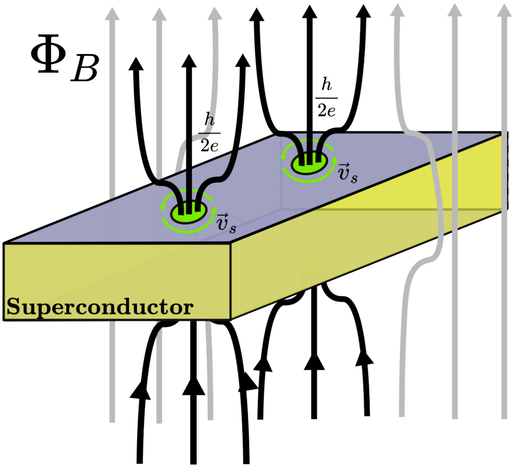

Figure 1.6: Schematic representation of a type-II superconductor in a magnetic field. The figure shows the magnetic flux-lines penetrating the superconducting sample through vortices. Each vortex carries a single ϕ_0 flux quanta and exhibits a circulating supercurrent flow $\vec{v_s}$.

In the gapped regime of the Fu-Kane model, vortex defects trap a special type of zero-energy excitation called Majorana zero-modes. These quasi-particles are unique in that they are their own antiparticles. Although they were originally predicted in particle physics to describe neutrinos, they can also appear in condensed matter systems as a consequence of particle-hole symmetry. This is an anti-unitary symmetry that anticommutes with the Hamiltonian, resulting in eigenstates of a Bogoliubov-de Gennes Hamiltonian that are symmetric around zero energy. While eigenstates will generally occur in pairs around zero energy, a single zero-energy excitation cannot be gapped as long as the symmetry is preserved, resulting in isolated zero-energy excitations known as Majorana quasi-particles. These quasi-particles are eigenstates of the particle-hole symmetry and appear as equal superpositions of electrons and holes. To form a complete basis, such states always appear in pairs. Although this may appear to nullify their protection, they can be strongly spatially separated, allowing for protection against splitting from E=0 symmetrically in pairs. Majorana operators can be defined from their fermionic counterparts as

$$\gamma_1 = c^\dagger + c = \gamma_1^\dagger \tag{1.11}$$

$$\gamma_2 = i\big(c^\dagger - c\big) = \gamma_2^\dagger. \tag{1.12}$$

Because these operators are their own Hermitian conjugates, they exhibit a special commutation relation

$$\big\{\gamma_i, \gamma_j\big\} = 2\delta_{i,j}. \tag{1.13}$$

When these properties are combined, it turns out that Majorana zero-energy excitations exhibit non-abelian exchange statistics. This means that, unlike fermions and bosons, an exchange of Majoranas can fully change the quantum state. This unique property, combined with their strong protection, can be used in quantum computation to generate stable topological qubits that are protected from all local decoherence effects. Therefore, it is crucial to explore and discover viable new systems where Majorana zero-energy excitations can appear.

In the case of the Fu-Kane model, these Majorana states are bound to the vortex cores. Each vortex binds an exponentially localized zero-energy solution. These states appear in the presence of a magnetic field inside the superconducting gap, with a degeneracy equal to the number of flux quanta, $N = \phi/\phi_0$.

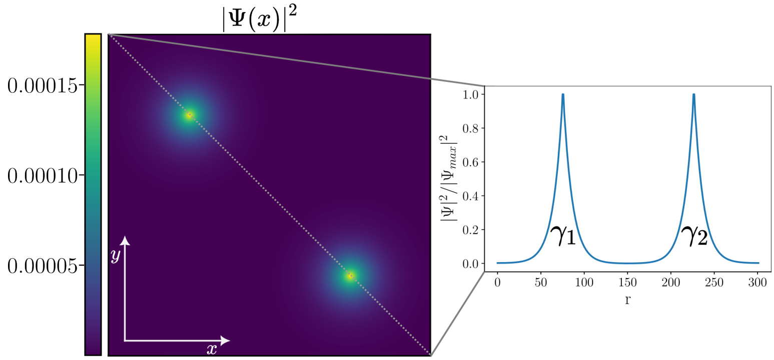

Figure 1.7: Probabilty density for zero mode solutions in a Fu-Kane superconductors. Majorana zero-modes are bound to the vortices of a superconductor with a characteristic exponential decay.

While these are the characteristic excitations in the gapped regime, it is known that the Fu-Kane superconductor becomes gapless in the presence of a strong supercurrent. We have shown that such gapless points exhibit a special type of zero-energy Landau levels. However, it turns out that this is not always the case for superconducting systems. Even though the magnetic field can become almost homogeneous in a sufficiently dense vortex lattice, the vortices still act as scatterers, which generally broadens the predicted zeroth Landau level[16].

In this thesis, we will present an example where a special symmetry prevents this broadening. We will demonstrate that the Fu-Kane model exhibits a unique type of symmetry called chiral symmetry. This is a local unitary symmetry that anti-commutes with the Hamiltonian. It allows us to write the Hamiltonian in a distinctive off-diagonal form described by

$$H_{chiral} = \begin{pmatrix} 0 & \Xi \\ \Xi^\dagger & 0 \end{pmatrix}. \tag{1.14}$$

This special form of the Hamiltonian enables us to invoke a theorem known as the Index theorem [17]. This theorem tells us that chiral Hamiltonians exhibit a unique integer value known as the index. This index can be calculated from the matrices Ξ and $\Xi^\dagger$ by looking at their corresponding kernels. While the dimensionality of the kernels (number of zero modes) of each of these two matrices can vary strongly, it turns out that their difference is very robust. This difference then defines the index, a topological invariant that cannot change under smooth local perturbation. Moreover, this invariant directly corresponds to the total number of zero-modes in the system. Therefore, as long as the chiral symmetry is preserved, the number of zero-modes is conserved by a special topological protection. In this thesis, we will demonstrate that this invariant can not only predict the Majorana zero-modes, but remains unchanged when the Fu-Kane model transitions to the gapless regime. We will show how this leads to a new zero-energy superconducting state, where Majorana states delocalize into an extended Landau level state.

1.4 Weyl fermions in Kramers-Weyl semimetals

The concept of massless fermions can be extended to three dimensions, where they are known as Weyl fermions. These are found in specific systems called Weyl semimetals [13]. In a two-band theory of a three-dimensional crystal, there are no possible perturbations that could gap out a Weyl cone. This is due to the fact that a three-dimensional Dirac equation requires a four-dimensional representation to describe massive particles. Thus, the protection of the gapless Weyl points is much stronger, as they can only couple in pairs with opposite chirality. As we will later see, they are protected by a topological number directly related to the chirality of the Weyl fermion. This means that systems exhibiting Weyl fermions, unlike Dirac systems, do not require an additional symmetry; they only require pairs of Weyl fermions to be well separated. Such pairs are then reconnected on the surface of Weyl semimetals with a special class of two-dimensional surface states called Fermi arcs.

As Weyl cones in nature always appear in pairs of opposite chirality, Weyl semimetals need to either break time-reversal or inversion symmetry. This allows pairs of Weyl cones in momentum space to be split so that gapless points do not overlap. While there are many different realizations of Weyl fermions in nature, this thesis will focus on newly described systems that exhibit Kramers-Weyl fermions [9, 10]. These occur in crystals with preserved time-reversal symmetry but broken inversion symmetry. We have found new unique signatures of these novel states, specifically a new type of magneto-oscillations that arise as a consequence of characteristic long Fermi arcs as well as unique spectral statistics. To introduce this work, we will first discuss the general protection of three-dimensional gapless Weyl nodes. We will then focus on the specific form of Kramers-Weyl systems. Finally, we will explain the idea of Fermi arcs as one of the characteristic signatures of three-dimensional massless fermions and explain their special extended form inside Kramers-Weyl semimetals.

1.4.1 Topological protection

As previously mentioned, the protection of Weyl points, unlike Dirac cones, does not require additional symmetries. This can be easily understood by examining the Weyl Hamiltonian, which shows that any perturbation that maintains translation symmetry will simply shift the Weyl cones in momentum space, while keeping a linear dispersion $E_{\text{Weyl}} \pm \sqrt{(k_x - V_x)^2 + (k_y - V_y)^2 + (k_y - V_y)^2}$ without introducing an effective mass.

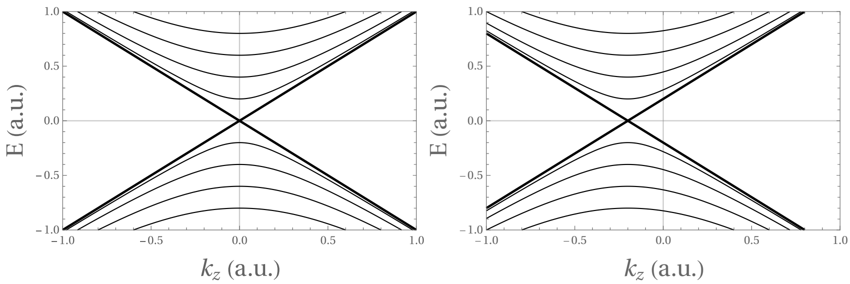

Figure 1.8: Gapless dispersion of a Weyl fermion. Left panel shows a Weyl cone in the center of the Brillouoin zone while the right panel shows a cone shifted in momentum space by a $V_z\sigma_z$ perturbation.

This type of protection is indeed very strong and quite peculiar, as we know that there must exist an atomic limit in which any system becomes strongly gapped. It is possible to achieve such a limit by coupling together two Weyl fermions, as is done in a four-dimensional representation of the Dirac equation. This process is naturally resolved in nature, as Weyl fermions can only appear in pairs. This allows the Weyl point to gap out, giving us a fully gapped dispersion $E_{\text{massive}} = \pm\sqrt{k_x^2 + k_y^2 + k_z^2 + M^2}$ that arises from the four-band Hamiltonian

$$H_{\text{Massive}} = \tau_z(\vec{\sigma} \cdot k) + \tau_x M. \tag{1.15}$$

Here the τ Pauli matrices describe the different Weyl cones, with τ_z representing two Weyl fermions with opposite chiralities, which plays an important role in the gap opening mechanism.

We can rewrite this argument independently of the exact form of the Hamiltonian by defining a topological invariant that characterizes each

Weyl cone and its protection. To do so, we must examine the behavior of the Berry curvature

$$\Omega_n(\vec{k}) = \nabla_k \times \mathcal{A}_n(R), \tag{1.16}$$

which takes the form of a quasi-magnetic field arising from the Berry connection $\mathcal{A}_n$. Such quasi-magnetic field defined by the Berry curvature acts as a magnetic monopole around the Weyl points, with the charge of such a monopole depending on the chirality of the Weyl fermion. As this charge takes discrete values, we know that no perturbation can remove it in a continuous manner. This charge therefore defines a topological invariant that tells us that such a Weyl point cannot be removed by itself. The only way to cancel out the monopole of the Berry curvature is to combine it with an additional monopole of opposite charge. This argument agrees with our previous prediction but is less reliant on the exact shape of the Hamiltonian. It tells us that as long as our system exhibits such unmerged monopoles in the Berry connection, the corresponding Weyl points will remain protected.

To summarize, the protection of Weyl points does not require additional symmetries, and it is a strong and peculiar type of protection. Coupling together two Weyl fermions can lead to a fully gapped dispersion, while the behavior of the Berry curvature provides a topological invariant that characterizes the protection of each Weyl cone.

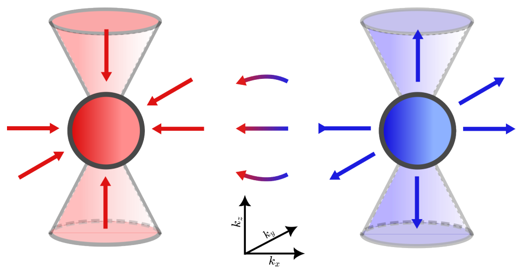

Figure 1.9: A schematic of the reconnection of two opposite monopoles of the Berry connection around the Weyl points.

1.4.2 Kramers-Weyl semimetal

We will now focus on a specific realization of Weyl fermions that occurs in Kramers-Weyl semimetals. Such systems are very exciting as they can not only provide a new approach to discovering materials described by

Weyl physics but also exhibit new characteristic behavior that is absent in conventional Weyl semimetals. This new type of massless excitation arises as a consequence of the preserved time-reversal symmetry. Specifically, we know that time-reversal symmetric systems exhibit a special degeneracy at time-reversal invariant points known as the Kramers degeneracy. This means that we can find gapless points at each corner of the three-dimensional Brillouin zone. As most crystals are invariant under inversion symmetry, which relates $E_{\uparrow}(k) = E_{\uparrow}(-k)$, the expansion around the gapless form must be even in momentum. This usually results in fully doubly degenerate bands around corners of the Brillouin zone with an effective quadratic dispersion.

However, we can focus on special chiral crystals that break inversion symmetry while still preserving time-reversal symmetry. These systems still have Kramers doublets at all the corners of the Brillouin zone but now exhibit a linear $\vec{\sigma}\cdot\vec{\delta k}$ expansion that describes Weyl excitations. This implies that all effective two-band models with time-reversal symmetry that break inversion symmetry will exhibit Weyl fermions at all the time-reversal invariant points in the Brillouin zone.

While this statement seems very robust, it turns out that while these Weyl cones are guaranteed to exist, they may not be easy to observe. This is because of two additional properties of such systems. First, the Weyl nodes can be strongly spread out in energies and can be quite far away from the Fermi surface. Second, our arguments arise from the expansion of the Hamiltonian for small momentum around the special degenerate points. While this expansion is generally linear, nothing forbids the appearance of higher-order quadratic terms. This means that the Kramers-Weyl cones are well-defined on the momentum scale where the linear term remains the governing part of the expansion. In reality, this tells us that we must consider systems that exhibit strong spin-orbit coupling in addition to the given prescription to study this novel realization of Weyl fermions.

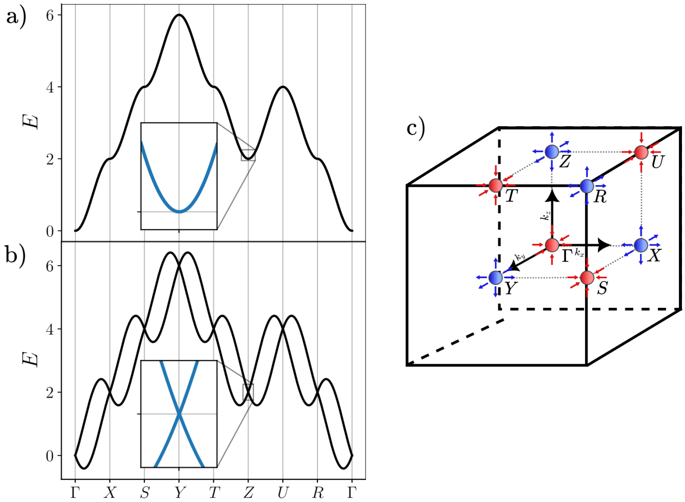

Figure 1.10: A schematic example of a generic two band dispersion for a) preserved, b) broken inversion symmetry. c) Schematic of the Kramers-Weyl Brillouin zone, identifying the time-reversal invariant momenta and their coresponding Weyl cones.

Now that we have understood the mechanisms responsible for the emergence of Kramers-Weyl fermions, it is important to explore the distinguishing features of these systems as compared to conventional Weyl semimetals. As we have already mentioned, Weyl fermions can only appear in pairs of opposite chiralities in nature. In contrast to a conventional three-dimensional semimetal, which typically hosts one or two pairs of massless fermions, Kramers-Weyl semimetals always exhibit four pairs of Weyl fermions with alternating chiralities. Since all these cones are precisely located at time-reversal-invariant momenta, they are guaranteed to have a strong separation in momentum space. This not only confers them with unusual robustness but is also quite distinct, as it is generally difficult to strongly pair Weyl fermions in the Brillouin zone. The large separation of the cones is responsible for unique signatures, as it forces the Fermi arc surface states that connect the Weyl cones to span over the entire Brillouin zone.

1.4.3 Fermi arcs

We have demonstrated that each Weyl point carries a topological invariant representing the monopole charge of the Berry connection. In the bulk, such a monopole can only annihilate with its opposite partner, providing a mechanism for continuously transforming the Weyl system into the atomic limit where the system is fully gapped. Alternatively, we can consider a sharp interface where we truncate the Weyl semimetal, creating a contact with the surrounding vacuum. As the Weyl system exhibits pairs of monopoles and the vacuum does not, these monopoles have to recombine on the interface during the transition from the Weyl semimetal to the vacuum. As a consequence, Weyl semimetals have to exhibit special types of surface states that connect Weyl cones of opposite chiralities and annihilate the monopole charges. These states are called Fermi arcs, as they form special two-dimensional Fermi surfaces. They are massless states with linear dispersion and are one of the characteristic signatures of Weyl semimetals.

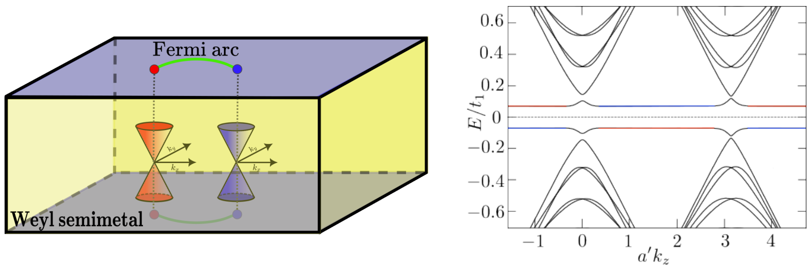

Figure 1.11: Left panel: Schematic representation of the Fermi arc surface states reconnecting the Bulk Weyl cones. Right panel: A dispersion of a Kramers-Weyl semimetal in a slab geometry showing the characteristic long Fermi arcs spanning the whole Brillouin zone.

The signature of such surface states is directly related to the separation of Weyl cones, as the Fermi arcs exhibit a higher density of states when they span over a larger region of the Brillouin zone. For this reason, Kramers-Weyl semimetals can be a good platform for their study, as they guarantee a large momentum space separation. Additionally, it turns out that unlike in conventional Weyl semimetals, Fermi arcs in Kramers-Weyl materials create a new type of periodic Fermi surface structure, where open orbits can form, giving us a completely unique magnetic behavior.

1.5 Outline of this thesis

This thesis covers a diverse range of massless electronic systems, which can be broadly divided into three parts. The first part focuses on the study of Dirac fermions and their properties. The second part focuses on the three-dimensional crystals and the signatures of Weyl physics. Finally, the thesis concludes with the last two chapters that concentrate on superconducting Majorana excitations.

1.5.1 Part 1

This part delves into the localization properties of two-dimensional massless fermions. We explore various condensed matter systems that exhibit Dirac fermions and propose a novel technique for the study of Anderson localization.

Chapter 2: Localization landscape of Dirac fermions

Non-interacting systems under the presence of random disorder exhibit universal behavior called Anderson localization. This means that electronic wave functions become strongly localized, impairing transport properties in the system. While it is generally impossible to find all the localization centers without diagonalization, it turns out that it is possible to define a special function that is strongly sensitive to the localized behavior of low-energy states. This function is called the Localization landscape and it can be efficiently calculated for a Schrödinger equation of spinless electrons with a positive definite Hamiltonian. In this chapter, we have extended this idea to spinful systems described by the Dirac equation. In particular, we have concentrated on systems with strong spin-orbit coupling to be able to study localization in graphene, topological insulators, and superconductors. We use the Ostrowski comparison matrix to treat systems that are not positive definite and extend the localization landscape bound to their comparison matrix. This defines a new landscape that can be efficiently calculated by solving the $Hu(r) = 1$ differential equation, where H is the comparison matrix of a chosen Dirac Hamiltonian. As the comparison matrix is only sensitive to real Hamiltonian elements, we were able to define a new equivalence class for Anderson localization. This allows us to find equivalent Hermitian and non-Hermitian Hamiltonians that share the same localization properties.

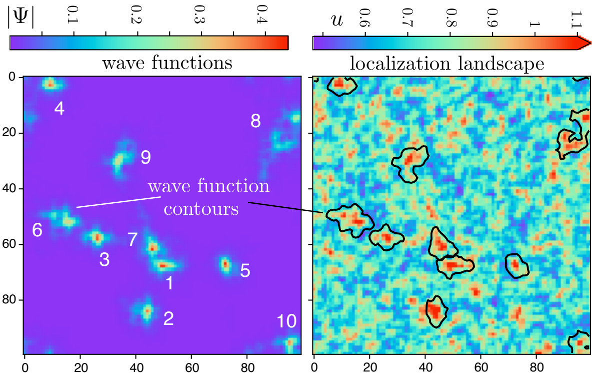

Figure 1.12: Localization centers of a disordered Dirac system (left) compared to the comparison matrix Localization landscape predictions (right).

1.5.2 Part 2

The second part of this thesis focuses on the behavior of Weyl fermions in the presence of a magnetic field. Specifically, we will investigate two systems and examine new signatures of Kramers-Weyl fermions as previously described in the introduction. Additionally, we will explore the transport properties of Landau levels in Weyl superconductors.

Chapter 3: Magnetic breakdown spectrum of a Kramers-Weyl semimetal

Kramers-Weyl semimetals exhibit four widely separated pairs of Weyl fermions at time reversal invariant points. In a finite sample, they give rise to unique extended Fermi arcs that span through the whole Brillouin zone. This chapter will focus on the consequences of the interplay between such characteristic surface states and a magnetic field. In particular, we show that the long Fermi arcs can form open orbits in momentum space. In the presence of a magnetic field, these can interact and couple with the Landau levels formed from the closed orbits in the bulk, thereby broadening their dispersion relation. We can use an effective model to describe this behavior in terms of a one-dimensional superlattice induced by the magnetic breakdown. Such a model can predict resonant behaviors when the dynamics are dominated by either open or closed orbits. This resonant behavior can be observed in terms of $1/B$ periodic magneto-oscillations, which are fully unique to the Kramers-Weyl semimetals compared to the usual Shubnikov-de Haas oscillations that arise from Landau level quantization.

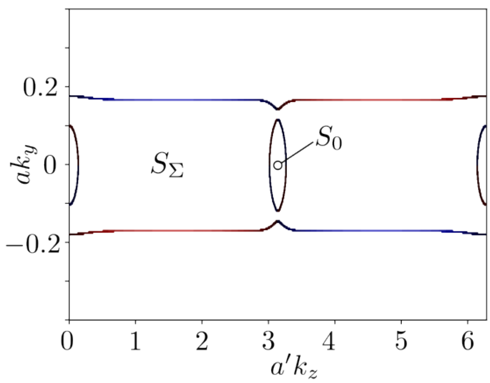

Figure 1.13: Figure shows the characteristic Fermi surface of a Kramers-Weyl semimetal in a slab geometry, focused around a single Weyl cone. Such Fermi-surface exhibits both open and closed orbits in the momentum space.

Chapter 4: Supercell symmetry modified spectral statistics of Kramers-Weyl fermions

In this chapter, we continue to investigate the unique signatures of Kramers-Weyl fermions. Using the predictions of random matrix theory, we explore the spectral statistics of a Kramers-Weyl toy model given by $H = v\sum_\alpha \sigma_\alpha \sin k_\alpha + t\sigma_0 \sum_\alpha \cos k_\alpha$ in a chaotic quantum dot. We find a hidden symmetry in the limit of small t that mimics a spinless time-reversal symmetry. This is a consequence of a special supercell symmetry that holds exactly when $t = 0$. We examine the consequences of this additional symmetry by observing the level spacing distribution $P(\alpha s^\beta)$, where we find that the calculated spectral statistic for small t truly obeys the orthogonal $\beta = 1$ ensemble instead of the expected symplectic ensemble $\beta = 4$. While this hidden symmetry is quickly broken for any realistic values of t, we find that signatures of the transition can still be detected. In particular, we show that this transition happens much slower when we observe the transition from weak localization to weak antilocalization, providing us with a new probe to detect the Kramers-Weyl fermions.

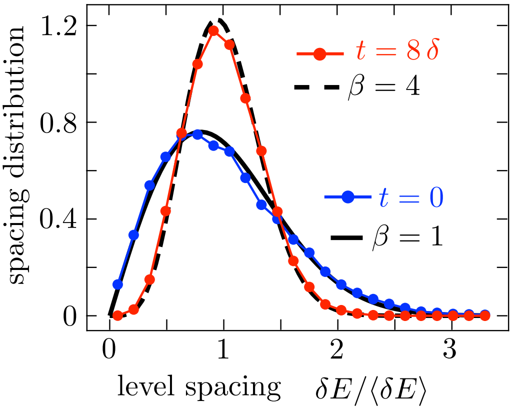

Figure 1.14: Two limiting examples of the spacing distribution comparing the orthogonal behaviour at small t and symplectic behaviour for large t.

Chapter 5: Chiral charge transfer along magnetic field lines in a Weyl superconductor

A heterostructure consisting of alternating layers of a Weyl semimetal and a conventional superconductor creates a gapless superconducting system called a Weyl superconductor. It was recently shown that, unlike conventional gapless superconductors, these systems exhibit a protected zeroth Landau level in the presence of a magnetic field. This chapter follows up on the recent study of the conductance signatures of these superconducting Landau levels. We have found a new conductance signature where the conductance depends on the direction of the magnetic field compared to the chiralities of the Weyl cones. This gives us a novel signature that can directly probe the chiralities of superconducting Weyl fermions.

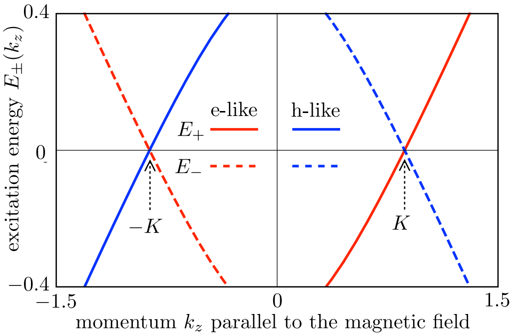

Figure 1.15: Dispersion relation of the superconducting zeroth landau level in the direction parallel to the magnetic field.

1.5.3 Part 3

The final section of this thesis will concentrate on the emergence of Majorana fermions. Specifically, we will investigate the Fu-Kane heterostructure introduced earlier and study how the interaction between the magnetic field and supercurrent can displace Majorana fermions away from the vortex cores.

Chapter 6: Deconfinement of Majorana vortex modes produces a superconducting Landau level

Shared contribution with Michał Pacholski; I was responsible for the numerical simulations.

A Fu-Kane superconductor in the presence of a magnetic field binds Majorana zero-energy excitations to the cores of the magnetic vortices. These are strongly localized excitations, topologically protected because of their exponentially small overlaps. This chapter examines how such protected states behave in the presence of a strong supercurrent, which can be interpreted as a spatially oscillating pair potential $\Delta(\vec{r}) = \Delta_0 e^{2i\vec{K}\cdot\vec{r}}$ describing Cooper pairs with momentum $\vec{K}$. We show that such a supercurrent induces a delocalization transition when $K > \Delta_0/\hbar v$, extending the Majorana modes into a new fully delocalized state with a unique oscillatory pattern. Using the index theorem, we prove that at $\mu = 0$, these states surprisingly remain gapless despite their strong overlaps. In fact, they form a dispersionless superconducting Landau level that is fully protected from broadening by the inter-vortex scattering. We then find an exact analytical solution for this new superconducting state and calculate the characteristic wave vector as $\sqrt{K^2 - (\Delta_0/\hbar v)}$. We show that this striped pattern can be used to measure the chirality of Majorana fermions and propose a local density of states measurement to investigate such states experimentally.

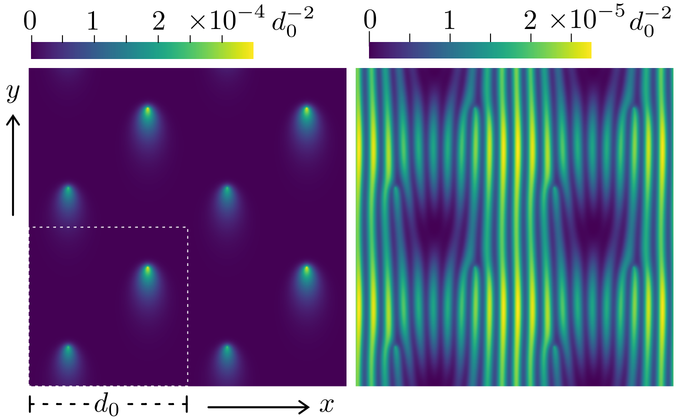

Figure 1.16: Two plots show the transition in the local density of states, induced by the supercurrent, for a Fu-Kane model with a vortex lattice. The first image is showing the strongly localized Majorana solutions at small supercurrent momentum $\Delta_0 < K/\hbar v$ while the second image shows the new strongly oscillating extended states at $\Delta_0 > K/\hbar v$.

Chapter 7: Magnus effect on a Majorana zero-mode

In the last chapter, we will continue studying the newly discovered delocalization transition of Majorana zero-modes in the Fu-Kane model. Specifically, we will examine how the dynamics of delocalization can manifest as a manifestation of the Magnus effect. In our system, this effect arises from the coupling between the superflow and the velocity profile inside the vortex core. This effect induces an acceleration on the Majorana vortex modes perpendicular to the superflow. As the supercurrent velocity profile around the vortex core depends on the chirality, if the supercurrent is strong enough, it can induce a full escape where the localized Majorana modes propagate away from the vortex core in the form of a localized wave-packet with a constant velocity. This effect is extremely surprising as, unlike the magnetic field, it is actually inducing a force on chargeless Majorana states that do not feel the conventional Lorentz force. We demonstrate this effect numerically by simulating a quench of the superflow. Furthermore, we find a semiclassical description for the wave packet that allows us to predict and match the final velocity of this escape regime.

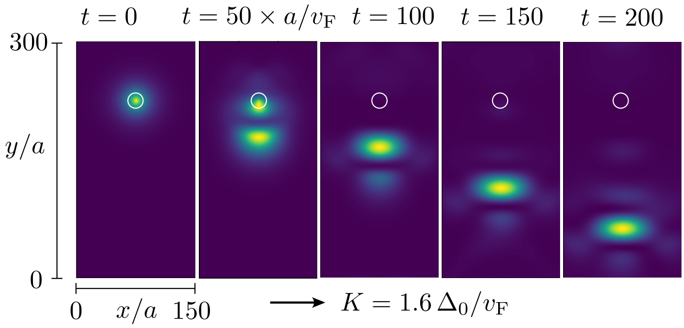

Figure 1.17: The escape behaviour of the chragless Majorana zero-modes under the influence of a strong superflow. The figure shows the propagation of the wave packet in a straight trajectory defined by chirality in the plane perpendicular to the superflow.